Kinetic and Spectroscopic Properties of the $Y_Z^{\bullet}$ Radical in Ca^{2+}- and Cl^--Depleted Photosystem II Preparations†

Nikos Lydakis-Simantiris,‡,§,|| Pierre Dorlet,‡,⊥ Demetrios F. Ghanotakis,§ and Gerald T. Babcock*,‡

Department of Chemistry, Michigan State University, East Lansing, Michigan 48824, and Department of Chemistry, University of Crete, P.O. Box 1470, 71409 Iraklion, Crete, Greece

Received December 4, 1997; Revised Manuscript Received March 4, 1998

ABSTRACT: Depletion of Ca^{2+} and/or Cl^- ions from PSII membranes blocks the electron-transfer reactions that precede O_2 evolution on the oxidizing side of the enzyme. Illumination of these inhibited preparations at 273 K generates a paramagnetic species that is detectable by low-temperature (T < 20 K) EPR as a signal in the $g = 2$ region, 90−230 G wide, depending on the treatment that PSII has undergone. This signal has recently been assigned to $Y_Z^{\bullet}$ in magnetic interaction with the manganese cluster in its S_2 state [Gilchrist et al. (1995) *Proc. Natl. Acad. Sci. U.S.A. 92*, 9545−9549]. This view, however, is not universal, owing, in part, to the fact that its spectroscopic properties depend on the preparation and the experimental conditions used for its study and, in part, to uncertainties as to the room temperature behavior of $Y_Z^{\bullet}$ in inhibited preparations. Here, we report time-resolved and conventional EPR data showing that, at room temperature and at 273 K, $Y_Z^{\bullet}$ can be accumulated in its 20 G form in high yields in both Ca^{2+}-depleted and acetate-inhibited preparations, and that the kinetics of its decay match the decay kinetics of the low-temperature signal generated in corresponding samples. The properties of the $Y_Z^{\bullet}$ signal, however, are shown to depend on the polypeptide content, the temperature, and the electron donors and acceptors present in the sample under examination. Our results support assignment of the EPR signal in inhibited preparations to S_2 $Y_Z^{\bullet}$ and demonstrate a protective role of the 17 and 23 kDa extrinsic polypeptides for the manganese cluster against externally added reductants.

Oxidation of water with concomitant production of molecular oxygen as a byproduct takes place in photosystem II (PSII),[1] a multipolypeptide enzyme in higher plants, algae, and cyanobacteria (for reviews, see *1*−*5*). Two molecules of substrate water bind to a cluster of four manganese ions and, after accumulation of 4 oxidizing equiv (*6*), one molecule of oxygen is released. The five distinct redox states of the manganese cluster are known as the S_n states (n = 0−4). During each step of this cycle, P_{680}^+, the oxidized form of the photoactive chlorophyll complex of PSII, is rereduced by Y_Z, a tyrosyl residue located at the 161 position of the D1 protein. The product of this electron-transfer reaction, $Y_Z^{\bullet}$, is a neutral radical (*7*), which interacts with the manganese cluster so that the transfer of an oxidizing equivalent occurs, advancing the S-state of the cluster and regenerating the Y_Z species. Recent data suggest that Y_Z is part of the OEC and participates directly in electron/proton-transfer reactions in oxidizing substrate water (*4*, *8*−*13*). There is an additional redox-active tyrosyl residue, known as Y_D, located at the 160 position of D2 protein, with an unclarified role (*14*, *15*). The oxidized form of this radical, $Y_D^{\bullet}$, is responsible for a stable EPR signal that is almost identical to that of the transient $Y_Z^{\bullet}$ signal (*14*).

There is agreement that, during each of the first two steps in the Kok cycle ($S_0 \rightarrow S_1$ and $S_1 \rightarrow S_2$), 1 oxidizing equiv is stored on the manganese cluster in the OEC (for reviews, see *1*, *4*). For the $S_2 \rightarrow S_3$ transition, opinion is divided between accumulation of the third oxidizing equivalent on the manganese cluster (*11*, *16*−*18*) and the oxidation of a different moiety, either a histidine (*19*−*23*) or a bridging oxo, in the cluster (*5*; see also *24*, *25*). For the final, $S_3 \rightarrow [S_4] \rightarrow S_0$ step, the reduction of $Y_Z^{\bullet}$ occurs with the appearance of O_2, which implicates $Y_Z^{\bullet}$ directly in the O═O bond forming chemistry (*11*).

Besides the cofactors directly involved in the redox reactions in the Kok cycle, two inorganic cofactors, Ca^{2+} and Cl^-, are necessary for enzyme function (for reviews, see *1*, *26*, *27*). In the absence of either of these cofactors, PSII can advance no further than the S_2 state (*28*−*33*). Following formation of S_2 in cofactor-depleted preparations,

† This work was supported by NIH Grant GM37300 and by the USDA Competitive Research Grants Office.

* Corresponding author. Telephone +(517) 355-9715. Fax: +(517) 353-1793. E-mail: babcock@cemvax.cem.msu.edu.

‡ Michigan State University.

§ University of Crete.

|| Present address: Department of Biology, University of Michigan, Ann Arbor, MI 48109.

⊥ Present address: DBCM/SBE CEN Saclay, Bdf 532, 91191 Gif-sur-Yvette Cedex, France.

[1] Abbreviations: DCBQ, 2,6-dichloro-*p*-benzoquinone; EDTA, ethylenediaminetetraacetic acid; EGTA, ethylene glycol bis(β-aminoethyl ether)-*N*,*N*,*N*′,*N*′-tetraacetic acid; EPR, electron paramagnetic resonance; ESEEM, electron spin−echo envelope modulation; ESE ENDOR, electron spin−echo electron nuclear double resonance; fwhm, full width at half-maximum; MES, 2-(*N*-morpholino)ethanesulfonic acid; OEC, oxygen evolving complex; PPBQ, phenyl-*p*-benzoquinone; PSII, photosystem II; P_{680}, special chlorophyll dimer of the reaction center; SDS−PAGE, sodium dodecyl sulfate−polyacrylamide gel electrophoresis; sw, salt washed; swpr, salt washed and protein reconstituted; Tris, tris(hydroxymethyl)aminomethane; XAS, X-ray absorption spectroscopy; Y_D, tyrosine 160D2; Y_Z, tyrosine 161D1.

S0006-2960(97)02980-2 CCC: $15.00
Published on Web 04/14/1998

room temperature illumination is reported to cause oxidation of Y_Z to produce $Y_Z^\bullet$ in its 20 G EPR-detectable form (*30*, *31*, *33*−*35*). This conclusion, however, has been challenged, and the situation with respect to the behavior of Y_Z at room temperature in these preparations remains in dispute (*23*, *32*, *36*). Illumination also gives rise to a broad doublet EPR signal, detected at cryogenic temperatures, with a *g* value near 2 and a line width of 90−230 G. This signal was first detected by Rutherford and co-workers (*37*, *38*) and can be generated in Ca^{2+}- or Cl^--depleted samples by illumination at 273 K or after one or two saturating flashes. Similar signals have been detected after treatment of PSII membranes with ammonia (*31*), citrate (*39*), or acetate (*40*, *41*). Britt and co-workers provided strong evidence indicating that this split signal arises from a magnetic interaction between $Y_Z^\bullet$ and the manganese cluster in its S_2 $Y_Z^\bullet$ state (*10*, *42*). Junge and co-workers, however, disagree with this interpretation and suggest instead that an oxidized histidine residue accumulates in the final state produced by illumination in Cl^--depleted preparations (*21*, *23*, *59*). Thus, there are considerable uncertainties as to species produced by room temperature illumination of cofactor-depleted preparations, and to species that are observed by low-temperature EPR in illuminated, freeze-trapped samples.

The resolution of these discrepancies is essential, as they have significant implications for models for the structure and function of the oxidizing side of PSII, as well as for the mechanism of water oxidation. Spectroscopic studies of samples giving rise to the split signal revealed close proximity of the Mn cluster and $Y_Z^\bullet$ (*4*, *10*, *43*). These and other results (*8*) led to the development of new models for water oxidation that implicate $Y_Z^\bullet$ in coupled electron/proton-transfer reactions during the S-transitions cycle (*4*, *9*−*13*, *43*, *44*). Other models invoke histidine residues in the mechanism of water oxidation (*19*, *23*, *45*). The determination of the behavior of the $Y_Z/Y_Z^\bullet$ couple in Ca^{2+}- and Cl^--depleted preparations is central to deciding whether and which of these models is viable.

Here, we present data, at room temperature and 273 K, on the formation and decay of $Y_Z^\bullet$ and the split signals in PSII membranes treated with NaCl or acetate. The effects of extraction of the 17 and 23 kDa extrinsic polypeptides and of different electron donors and acceptors on the kinetic properties of $Y_Z^\bullet$ are also presented. Our data demonstrate that $Y_Z^\bullet$ occurs as a 20 G radical at room temperature in cofactor-depleted preparations, that the split signal observed at cryogenic temperatures and the $Y_Z^\bullet$ EPR signal observed at room temperature and 273 K correlate kinetically, and that the extrinsic polypeptides provide a barrier to exogenous reductants on the oxidizing side of PSII.

MATERIALS AND METHODS

Oxygen-evolving PSII membranes were prepared from fresh market spinach according to the BBY method (*46*) with the modifications described in (*47*). Typical oxygen evolution rates of these preparations, measured by a Clark type oxygen electrode with 600 μM DCBQ as electron acceptor, were 700−800 mmol of O_2 (mg of Chl)$^{-1}$ h^{-1}.

Calcium depletion was achieved by incubation of PSII membranes (0.5 mg of Chl/ mL) in 1.2 M NaCl, 0.3 M sucrose, 25 mM MES (pH 6.5) for 30 min in room light on ice, as described in (*48*), or by two dialysis steps in high and low NaCl concentrations, respectively, as described in (*37*). In both cases, EGTA was added to the buffers for chelating Ca^{2+} and other divalent cations potentially present. These two methods resulted in Ca^{2+}- and 17- and 23 kDa-depleted PSII membranes (hereafter called sw-PSII) and Ca^{2+}-depleted protein-reconstituted PSII membranes (swpr-PSII). Ca^{2+} depletion was carried out just before the EPR experiments. Reconstitution of the extrinsic proteins was checked by SDS−PAGE, by using the Laemmli system as described in (*49*). The oxygen-evolution activity of the calcium-depleted samples was 20−30% of the control, whereas addition of 20 mM $CaCl_2$ recovered the activity to at least 80% of the control. For the above preparations, reagents free from Ca^{2+} contaminations were used (Aristar, BDH Laboratory Supplies; [Ca^{2+}] <1 ppm, [Cl^-] <0.5 ppm).

Tris-washed samples were prepared by 30 min incubation of PSII membranes (0.5 mg of Chl/mL) in 1 M Tris (pH 8.0), 1.25 mM EDTA in room light on ice. The samples were then washed twice by centrifugation (40000*g*, 15 min), resuspended in 50 mM MES (pH 6.5), 0.4 M sucrose, 15 mM NaCl (SMN), and stored at −80 °C until used. Electron acceptors were added to the samples just before EPR experiments.

Acetate-treated samples were prepared as follows: PSII membranes immediately after their preparation were washed twice by centrifugation with 5 mM $Ca(OH)_2$, 0.4 M sucrose, 50 mM MES (pH 5.5), resuspended in the same buffer at a concentration of about 8 mg of Chl/mL, and stored at −80 °C until use. Just before the EPR experiments, samples were thawed and 5 M acetate solution (pH 5.5) was added up to a final acetate concentration of 500 mM. Then, 1 mM $K_3[Fe(CN)_6]$ and 1 mM $K_4[Fe(CN)_6]$ were added, and the samples were transferred either to a flat cell or to EPR tubes in the dark. The oxygen-evolution activity of the acetate-treated samples was about 10% of the intact sample. Addition of 20 mM $CaCl_2$ to the assay solution reactivated the inhibited sample to more than 90% of control rates.

EPR experiments were carried out on a Bruker ESP300E instrument equipped with an Oxford ESR900 continuous-flow cryostat. For room temperature and 273 K experiments, a TM cavity was used. Controlled nitrogen flow through an ethanol/dry ice bath and a dewar in the TM cavity was used to maintain 273 K. For low-temperature experiments, a TE cavity was used. For illumination at room temperature, either a 300 W projector lamp or a homemade xenon flash lamp (17 ms fwhm) was used to illuminate samples in the TM cavity. Light saturation of the samples was checked with neutral density optical filters. For illumination at 273 K, a light setup comprising two 300 W projector lamps, an ethanol/dry ice bath in a non-silvered dewar, and a temperature-controlled nitrogen gas line were used. Samples in calibrated EPR tubes containing 1 mM $K_3[Fe(CN)_6]$ and 1 mM $K_4[Fe(CN)_6]$ were illuminated for 10 s at 273 K and then were incubated in the dark for specified times before freezing in liquid nitrogen. Other conditions are described in the figure legends. Double integration of the EPR spectra was done by using the built-in software of the EPR instrument. For the time-resolved experiments, the EPR instrument and the flash lamp were triggered by a personal computer. Analysis of the time-resolved EPR kinetic traces was done with Origin v3.78 (Microcal Software, Inc.)

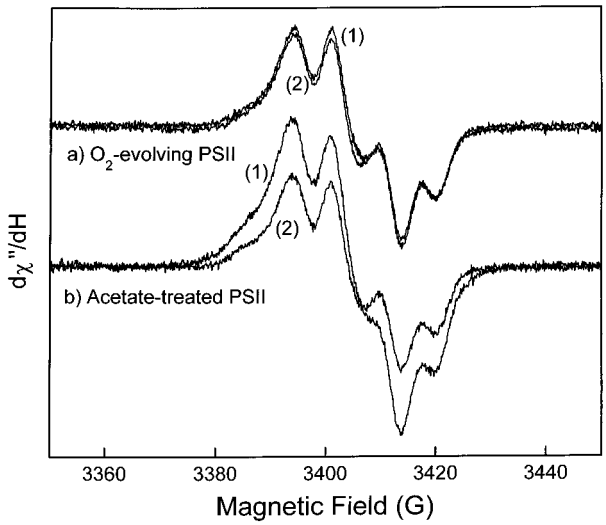

FIGURE 1: EPR spectra of $Y_Z^\bullet$ and $Y_D^\bullet$ recorded at room temperature. The spectra labeled (1) were recorded under continuous illumination, whereas the spectra labeled (2) were recorded in the dark after illumination. (a) Oxygen-evolving PSII membranes (6 mg of Chl/mL); (b) acetate-treated PSII membranes (6 mg of Chl/mL). The spectrum in the dark was recorded after 12 min dark-adaptation at room temperature. For all samples, 1 mM $K_3[Fe(CN)_6]$/1 mM $K_4[Fe(CN)_6]$ was used as the electron acceptor/redox buffer system. Other conditions: microwave power, 1 mW; modulation amplitude, 2.85 Gpp; time constant, 82 ms; gain, 4×10^5; sweep time, 336 s.

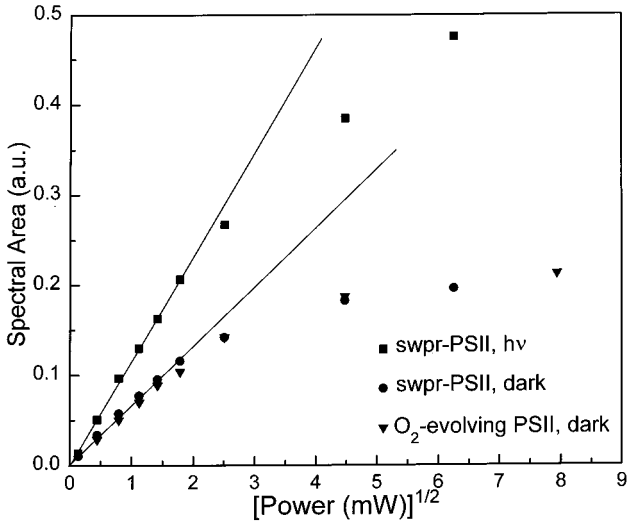

FIGURE 2: Power saturation curves of $Y_D^\bullet$ in O_2-evolving PSII membranes in the dark immediately after illumination (triangles) and of $Y_Z^\bullet$ and $Y_D^\bullet$ in swpr-PSII under continuous illumination (squares) and after 15 min dark adaptation at room temperature (circles). Each point is the average of three measurements. The sample concentration was 2 mg of Chl/mL, and 1 mM $K_3[Fe(CN)_6]$/1 mM $K_4[Fe(CN)_6]$ was used as the electron acceptor/redox buffer system. Experimental conditions: modulation amplitude, 2.5 Gpp; time constant, 164 ms; gain, 1.6×10^6; sweep time, 168 s.

RESULTS

Power Saturation of Tyrosyl Radicals in O_2-Evolving and Inhibited PSII Membranes. The light-induced radicals, $Y_Z^\bullet$ and $Y_D^\bullet$, give similar EPR signals (*7*, *14*). However, the relaxation properties of these two radicals differ, owing to differences in the distance between them and the manganese cluster, which acts as a strong relaxer. As $Y_Z^\bullet$ is closer to the manganese cluster, higher microwave power is required for saturation (*7*, *50*). Thus, power saturation measurements can be employed to discriminate between the two radicals, at least, for samples in which the manganese cluster is intact (*35*, *51*).

Figure 1 shows light-induced and dark EPR spectra at room temperature in O_2-evolving (a) and acetate-treated (b) PSII membranes. In the O_2-evolving sample, $Y_D^\bullet$ is dark-stable, and illumination does not produce a discernible increase in tyrosyl radical concentration, as the lifetime of $Y_Z^\bullet$ in O_2-evolving material is too short to allow its accumulation. In contrast, illumination of the acetate-treated sample produces a marked increase in signal intensity. Similar experiments were performed in sw- and swpr-PSII membranes with the same results (see below). Illumination of the samples with flashes at 2 Hz repetition rate, instead of continuous light, resulted in the same increase in signal intensity (data not shown).

The light-induced increase in tyrosyl radical intensity could arise from the induction of $Y_Z^\bullet$ in these inhibited samples (*31*, *33*, *34*) or from $Y_D^\bullet$ by modification of its power saturation properties (*32*, *36*). To resolve this issue, we performed power saturation studies, as shown in Figure 2, where the integrated areas of the dark- and light-induced signals are plotted as functions of the square root of power. The curve corresponding to intact PSII membranes in the dark immediately after 10 s illumination (triangles) represents the saturation behavior of $Y_D^\bullet$ at a concentration of one spin per reaction center. The saturation behavior of the tyrosyl radicals in swpr-PSII membranes under continuous illumination and after 15 min dark-adaptation at room temperature (squares and circles, respectively) is also shown in the Figure 2. The spectra observed in the 15 min dark-adapted samples had an integrated area corresponding to one $Y_D^\bullet$ spin per reaction center. The spectra of the illuminated samples showed an increase of their integrated area at all the microwave powers. The same sets of experiments were repeated on sw-PSII membranes and on acetate-treated membranes. Over the range of microwave powers examined, illumination of the samples inhibited by these methods resulted in an increase in spectral area analogous to that shown in Figure 2 for swpr-PSII membranes (data not shown).

In Figure 3, we show spectra of Ca^{2+}-depleted samples recorded at 200 mW, a microwave value which falls well into the linear region of the saturation curves for dark and illuminated samples in Figure 2. The dark spectra correspond to one spin per PSII from $Y_D^\bullet$; illumination generates additional spins relative to the dark-adapted sample. In the case of sw-PSII, the light-induced increase was 0.69 spin; for swpr-PSII, the light-induced increase was 0.72 spin.

The data in Figures 1−3 clearly establish that room temperature illumination of salt-washed PSII samples, with or without the extrinsic polypeptides, or of acetate-treated PSII samples, results in an increase in the observed tyrosyl EPR signal at microwave powers from 20 to 200 mW. Because the transition probabilities of $Y_D^\bullet$ and $Y_Z^\bullet$ are the same (*52*), we can quantify the increase in the integrated area of the signals obtained from inhibited PSII membranes under illumination. The slopes of the plots in Figure 2 for O_2-evolving PSII and for swpr-PSII membranes in the dark correspond to one $Y_D^\bullet$ spin per PSII. The increase in slope in the illuminated swpr-PSII sample indicates that an

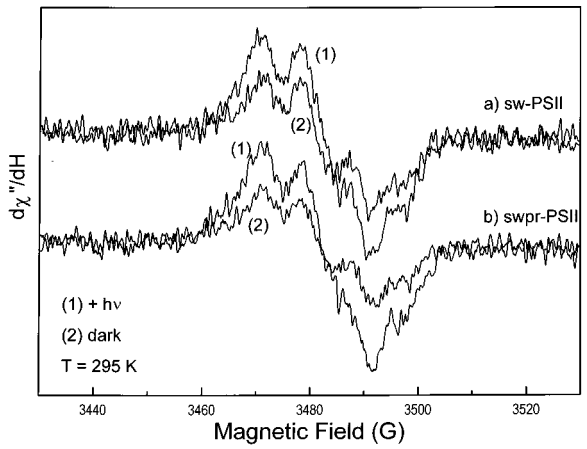

FIGURE 3: $Y_Z^\bullet$ and $Y_D^\bullet$ spectra from (a) sw-PSII and (b) swpr-PSII under continuous illumination (1) and after 15 min dark-adaptation at room temperature (2). Microwave power, 200 mW. Other experimental conditions as in Figure 2.

additional 0.75 spin is generated by light, and we attribute this to the generation of $Y_Z^\bullet$ in this preparation. In general, we find that 0.7−0.8 $Y_Z^\bullet$ spin/PSII in salt-washed samples and 0.6 $Y_Z^\bullet$ spin/PSII in acetate-treated membranes are generated in the light. The lower accumulation of $Y_Z^\bullet$ in acetate-treated samples may reflect incomplete removal of calcium and chloride ions, since the treatment took place by injection of acetate and not by washing the sample in acetate buffer. We conclude that Ca^{2+} depletion and acetate treatment generate states in which $Y_Z^\bullet$ can be photoaccumulated at room temperature in high yield (60−80%). After addition of $CaCl_2$, the O_2 evolution activity of the inhibited system is recovered more than 80%, and light-induced accumulation of $Y_Z^\bullet$ is no longer possible (see also below). This observation indicates that NaCl or acetate treatment of PSII membranes does not cause, in our hands, irreversible damage to the samples. Thus, we exclude the possibility that the light-induced $Y_Z^\bullet$ spins arise from Mn-depleted centers (see also below).

$Y_Z^\bullet$ Decay Depends on Experimental Conditions. Previous studies on the properties of PSII after depletion of its inorganic cofactors led to conflicting results (for example, see *32*, *33*). One of the controversies regards the decay kinetics observed by different groups for the light-induced tyrosyl radicals. We examined these kinetics in salt-washed PSII membranes with or without the 17 and 23 kDa extrinsic polypeptides and with various donors and acceptors. We monitored the reduction of the $Y_Z^\bullet$ radical by measuring the amplitude decay at the low-field peak in its EPR spectrum. During the optimization of the experimental conditions, we realized, in agreement with previous studies (*30*, *33*), that the decay of the signal was slow and that several flashes were needed to induce the maximum amount of spins. Thus, we could not average the kinetic traces produced by single flashes, as a very low repetition rate would be necessary. To overcome this problem, a single kinetic trace was recorded at high microwave power. Several flashes were necessary to maximize the $Y_Z^\bullet$ signal, which may indicate that a higher number of misses for the $S_1 \rightarrow S_2$ transition occurs in the absence of the inorganic cofactors. Use of high microwave power in order to increase the signal-to-noise ratio is valid, given the results in Figures 1−3 above, and does not affect the kinetic properties of the $Y_Z^\bullet$ radical.

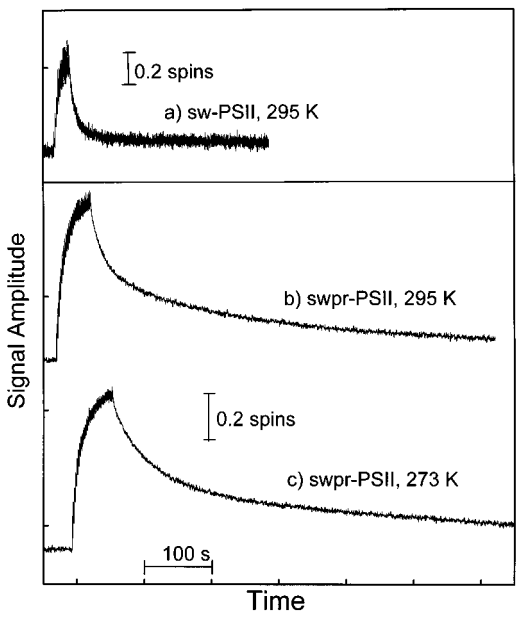

FIGURE 4: Kinetic traces of flash-induced $Y_Z^\bullet$ in (a) sw-PSII membranes at room temperature, (b) swpr-PSII membranes at room temperature, and (c) swpr-PSII membranes at 273 K. Experimental conditions: (a) microwave power 200 mW, modulation amplitude 2.5 Gpp, time constant 10.2 ms, gain 2.5×10^5, sweep time 336 s; (b) microwave power 200 mW, modulation amplitude 4.0 Gpp, time constant 82 ms, gain 1×10^6, sweep time 670 s; (c) as in (b) but sweep time 1342 s. 1 mM $K_3[Fe(CN)_6]$/1 mM $K_4[Fe(CN)_6]$ was used as the electron acceptor/redox buffer system.

Table 1: Half-Times of the Biphasic Decay of Signal II in the sw-PSII and swpr-PSII Membranes

sample	$t_{1/2\ fast}$ (s)	$t_{1/2\ slow}$ (s)
sw-BBYs, $K_3[Fe(CN)_6]/K_3[Fe(CN)_6]$, RT	4	40
sw-BBYs, DCBQ, RT	1.5	35
sw-BBYs, PPBQ, RT	2	26
swpr-BBYs, RT	20	140
swpr-BBYs, 273 K	35	320

In Figure 4 we present kinetic data taken from sw-PSII (a) and swpr-PSII membranes at room temperature (b) and at 273 K (c). Equimolar ferri- and ferrocyanide was used as the electron acceptor/redox buffer system. Kinetic trace (a) was taken at lower modulation amplitude, lower gain, and faster time constant so its amplitude is smaller and its signal-to-noise is lower than that in traces (b) and (c). To quantify the number of spins generated during the flash sequence, the initial amplitude under nonsaturating EPR conditions was compared with the amplitude of the fully oxidized $Y_D^\bullet$ signal under the same conditions (data not shown). Kinetic traces obtained at lower microwave power reproduced those shown in Figure 4; however, analysis of them was made difficult by the poor signal-to-noise.

Figure 4 shows that the decay of $Y_Z^\bullet$ in salt-washed PSII membranes depends on both the polypeptide content of the samples and the temperature. Analysis of the decays produced the half-life times given in Table 1. All traces showed biphasic behavior, in agreement with similar studies reported earlier (*30*, *31*, *33*). From these results, we conclude that the decay of the light-induced $Y_Z^\bullet$ becomes faster when the 17 and 23 kDa polypeptides have been removed and slows down further when the temperature is lowered to 273 K. In light of these results, we attribute the differences in decay kinetics reported by Andréason and co-workers (*33*)

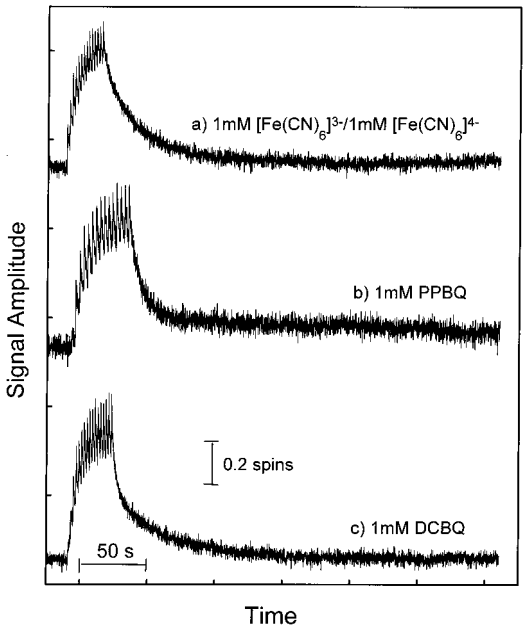

FIGURE 5: Kinetic traces of flash-induced $Y_Z^\bullet$ in sw-PSII membranes (2 mg of Chl/mL) at room temperature. Acceptors used: (a) 1 mM $K_3[Fe(CN)_6]$/1 mM $K_4[Fe(CN)_6]$; (b) 1 mM DCBQ; (c) 1 mM PPBQ. Instrument conditions as in Figure 4a.

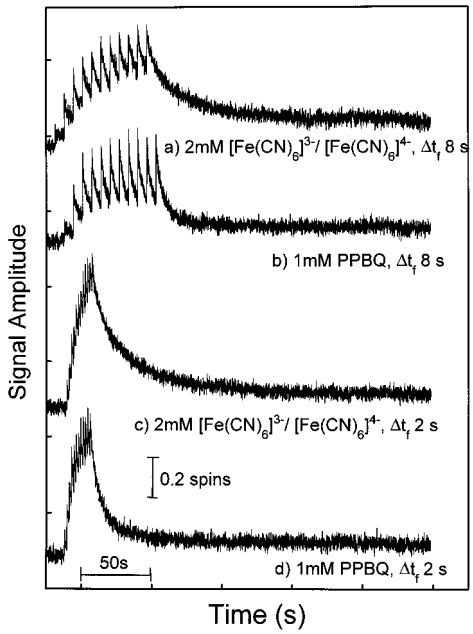

FIGURE 6: Kinetic traces of flash-induced $Y_Z^\bullet$ in sw-PSII membranes (2 mg of Chl/mL) at room temperature. Samples (a) and (c) contained 2 mM $K_3[Fe(CN)_6]$/2 mM $K_4[Fe(CN)_6]$, whereas samples (b) and (d) contained 1 mM PPBQ as electron acceptor. Flash frequency: (a) and (b), 0.125 Hz; (c) and (d), 0.5 Hz. Instrument conditions as in Figure 4a.

and Boussac and Rutherford (*32*) to differences in the experimental conditions used. Specifically, our study of $Y_Z^\bullet$ decay in sw-PSII membranes gave results similar to those of Andréasson et al. (*33*) in which extrinsic polypeptide-depleted samples were used. The kinetics of $Y_Z^\bullet$ decay we observed in swpr samples were, qualitatively, in agreement with those reported by Boussac and Rutherford (1995) in which PSII samples reconstituted with the 17 and 23 kDa polypeptides were used.

To investigate the effects of different experimental conditions on the decay of $Y_Z^\bullet$ further, we repeated the experiments in Figure 4 with different acceptors. These experiments are presented in Figure 5. The kinetics of $Y_Z^\bullet$ were monitored in sw-PSII samples that contained (a) 1 mM $K_3[Fe(CN)_6]$ and 1 mM $K_4[Fe(CN)_6]$, (b) 1 mM phenyl-*p*-benzoquinone (PPBQ), and (c) 1 mM 2,6-dichloro-*p*-benzoquinone (DCBQ). Effects of the electron acceptors on the decay of the $Y_Z^\bullet$ radical are apparent, and analysis of the traces provided the half-times summarized in Table 1. The hydrophobic acceptors DCBQ and PPBQ accelerated the reduction of the tyrosyl radical by 2−3-fold. The amplitude of the fast decaying phase after each flash was enhanced in the presence of these acceptors.

We addressed the origin of this fast decaying phase in an experiment in which the flash frequency was varied, being either 0.5 or 0.125 Hz. We also used two different acceptor systems, ferri-/ferrocyanide and PPBQ. The results for sw-PSII membranes are shown in Figure 6. Similar results were observed from swpr-PSII (data not shown). Kinetic analysis of the decays of $Y_Z^\bullet$ after each flash at 0.125 Hz (traces a and b) showed monophasic behavior with lifetimes corresponding to the fast phase of the decay of the full trace. The amplitudes of the traces taken with longer flash intervals are lower compared to the traces taken at higher flash frequency (traces c and d). This can be rationalized by the fact that between two flashes the number of $Y_Z^\bullet$ spins that decay is much higher at lower flash frequencies (compare traces after each flash in a and c and b and d).

An important conclusion from the data in Figure 6 and Table 1 is that the fast decaying phase observed at shorter flash intervals does not represent the decay of $Y_Z^\bullet$ from irreversibly damaged centers. If that were the case, we would expect to observe $Y_Z^\bullet$ decay kinetics similar to Tris-washed PSII membranes (20−40 ms under the conditions used, *53*). Moreover, we examined the kinetic traces of swpr-PSII with 1 mM DCBQ as the electron acceptor with two different time constants (10.2 and 82 ms) and found that the relative amplitude of the fast phase was the same in both. In another control experiment, we added 30 mM $SrCl_2$ or 30 mM $CaCl_2$ to sw-PSII membranes and examined the kinetics of the decay of the light-induced $Y_Z^\bullet$ radical under the same conditions as in Figure 5. The results are shown in Figure 7. We see that addition of 30 mM $SrCl_2$ resulted in a decrease of the photoaccumulated signal to about 40%, whereas addition of 30 mM $CaCl_2$ accelerated the decay of $Y_Z^\bullet$ so that it could not be detected with the 10.2 ms time constant used. We also recorded the $Y_Z^\bullet$ kinetics in salt-washed samples following addition of 30 mM $SrCl_2$ or 30 mM $CaCl_2$ under nonsaturating EPR conditions and obtained the same results (data not shown). These results are in agreement with the observation that addition of Ca^{2+} ions to salt-washed samples resulted in restoration of about 80% of the oxygen-evolution activity of the samples, and with the results of the $Y_D^\bullet$ spin count in active centers under nonsaturating conditions (see above).

The conclusions from the data in Figures 4−7 can be summarized. First, the decay rates of $Y_Z^\bullet$ depend on the extrinsic polypeptide content of the sample, the temperature, and the acceptor system. However, in all the cases, the decay is biphasic with the fast phase on the seconds time scale and the slow in minutes. This biphasic behavior may reflect

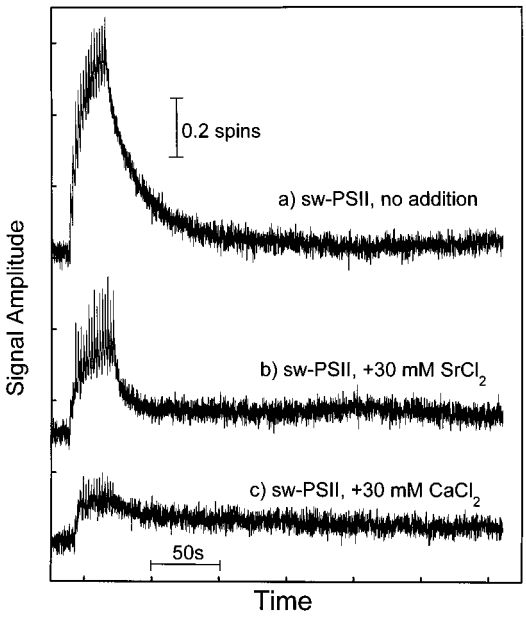

FIGURE 7: Kinetic traces of flash-induced $Y_Z^\bullet$ in sw-PSII membranes (2 mg of Chl/mL) at room temperature. All samples contained 1 mM $K_3[Fe(CN)_6]$/1 mM $K_4[Fe(CN)_6]$. (a) No additions, (b) 30 mM $SrCl_2$, and (c) 30 mM $CaCl_2$ were added to the sample just before the experiment. Instrument conditions as in Figure 4a.

the reduction of $Y_Z^\bullet$ via back-reactions from the acceptor side and by the reduced forms of the acceptors used. Second, regardless of the preparation or other conditions, $Y_Z^\bullet$ can be accumulated in high yields at room temperature either by continuous illumination or by flashes. Third, the blockage of electron transfer caused by NaCl or by acetate treatment is reversible upon addition of Ca^{2+} and/or Cl^- ions. The reactivated samples perform fast electron transfer upon illumination, so detection of $Y_Z^\bullet$ under the EPR conditions used for the inhibited samples is not possible.

Effects of Benzidine on $Y_Z^\bullet$ Decay. The effects of external reductants on the reduction of $Y_Z^\bullet$ were investigated in two different samples, namely, sw-PSII and swpr-PSII. Benzidine has been shown to be a very rapid and effective donor to PSII (*34*, *54*), and, accordingly, we used this reductant. A range of benzidine concentrations was used, and the results of these experiments are shown in Figure 8 A,B. For sw-PSII, we cannot detect $Y_Z^\bullet$ with a time constant of 10.2 ms, indicating very fast $Y_Z^\bullet$ reduction by this donor (Figure 8A). However, with swpr-PSII, accumulation of $Y_Z^\bullet$ was possible even in the presence of 100 mM benzidine (Figure 8B). The effect of benzidine on the decay of $Y_Z^\bullet$ was characterized by Ghanotakis et al. (*34*). In their study, they concluded that benzidine rereduces a higher S-state of the manganese cluster in the dark between flashes in a relatively slow process, and that the manganese cluster then rereduces $Y_Z^\bullet$ rapidly upon its photogeneration, as in the intact system. The results in Figure 8A,B agree with this mechanism, with the additional insight that the approach to the manganese cluster by benzidine depends on the 17 and 23 kDa polypeptides. Similar conclusions about the protective role of 17 and 23 kDa polypeptides have been made by Ghanotakis and coworkers (*55*). In their absence, benzidine has fast access to the manganese cluster and reduces it to S_1 or S_0 in the time between flashes. The light-induced $Y_Z^\bullet$ is rereduced by the manganese cluster with reaction lifetimes that correspond to the low S-state transitions. In the presence of the extrinsic

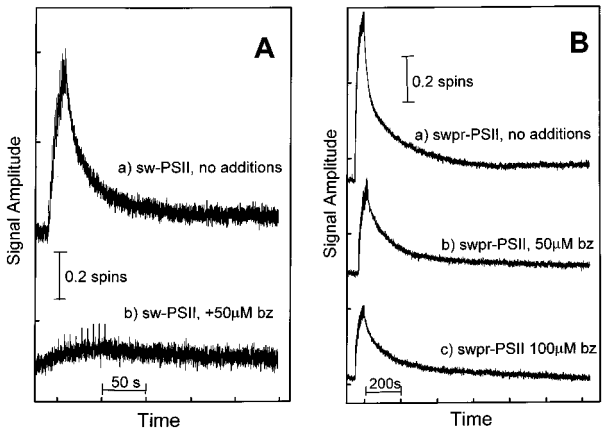

FIGURE 8: Effects of benzidine on the decay of $Y_Z^\bullet$ at room temperature in sw- (panel A) and swpr-PSII membranes (panel B). All samples contained 1 mM $K_3[Fe(CN)_6]$/1 mM $K_4[Fe(CN)_6]$. Panel A: (a) no additions; (b) 50 mM benzidine. Panel B: (a) no additions, (b) 50 mM benzidine, and (c) 100 mM benzidine were added to the sample just before the experiment. Other experimental conditions as in Figure 4a (panel A) or 4b,c (panel B).

polypeptides, access to the manganese cluster is hindered, and a smaller number of centers in the samples are reduced in the dark. Thus, accumulation of $Y_Z^\bullet$ is possible. The reduced amplitude of $Y_Z^\bullet$ when higher concentrations of benzidine are used supports that interpretation.

Relationship between $Y_Z^\bullet$ and the Split EPR Signal. Calcium and/or chloride depletion by NaCl and acetate treatment of BBY membranes cause the accumulation of $Y_Z^\bullet$ under illumination at room temperature, as shown above, and the formation of a split $g \approx 2$ EPR signal when treated membranes are illuminated at 273 K and then frozen to cryogenic temperatures (*19*, *40*, *41*). We examined the decay kinetics of both $Y_Z^\bullet$ and the split signal induced by illumination at 273 K of swpr-PSII membranes. We chose the extrinsic polypeptide sufficient system because of its slower $Y_Z^\bullet$ decay relative to sw-PSII (Table 1). The results are shown in Figure 9. In panel A, we present the split signals recorded after light generation at 273 K and subsequent dark incubation on ice for various times. Following the incubation period, the samples were frozen in liquid nitrogen and transferred to the cavity for EPR experiments at 15 K. We measured the signal amplitude at the low-field peak and plotted the values on the decay trace of $Y_Z^\bullet$ following flash illumination at 273 K (Figure 9, panel B). The first point, corresponding to the signal amplitude of the split signal with no dark-adaptation, was normalized in both axes in order to coincide with the onset of the $Y_Z^\bullet$ decay. The comparison, in panel B, clearly shows that the kinetics of $Y_Z^\bullet$ and split signal decay are the same. This result is qualitatively in agreement with similar results reported by Hallahan et al. (*31*) and by Brudvig and coworkers (*56*). The results in Figure 9 provide additional support for the interpretation of the split signal as originating from $Y_Z^\bullet$ in magnetic interaction with the manganese cluster in the S_2 state (*4*, *10*).

DISCUSSION

The properties of $Y_Z^\bullet$ were investigated at room temperature and 273 K in inhibited PSII membranes under a variety of experimental conditions. The inhibition was achieved

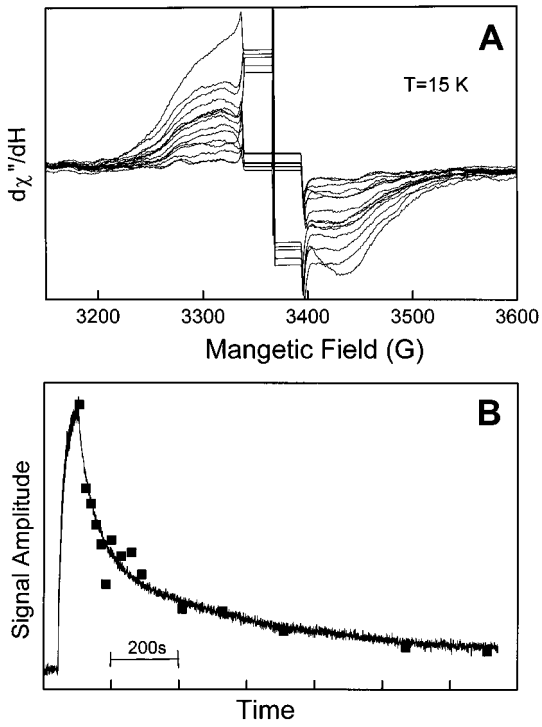

FIGURE 9: Effect of dark-adaptation on the amplitude of the split signal. Panel A: Light minus dark split signal spectra were recorded on swpr-PSII samples illuminated for 10 s at 273 K and then dark-adapted on ice for 0, 15, 30, 45, ..., 1200 s before freezing in liquid nitrogen (see panel B). EPR conditions: microwave power, 8 mW; modulation amplitude, 20 Gpp; time constant, 82 ms; gain, 8×10^4 or 1.6×10^5; temperature, 15 K. Panel B: The $Y_Z^\bullet$ decay trace of swpr-PSII membranes at 273 K (Figure 4c) is plotted along with the amplitudes of the low-field peak in the spectra in panel A vs the dark incubation time. See text for details.

either by treatment with high concentrations of NaCl or by addition of acetate. For all samples, we observed the accumulation of a 20 G wide tyrosyl radical by EPR during illumination at room temperature. Careful examination of the saturation properties of this radical signal allowed spin quantitation and showed that it arose from $Y_Z^\bullet$. We addressed the possibility that the $Y_Z^\bullet$ signal we observe in these preparations originates from irreversibly damaged centers that behave as Tris-washed material. Results from oxygen-evolution measurements and the data presented in Figures 6 and 7, however, ruled out that possibility.

These results agree with data published earlier on PSII membranes inhibited by various treatments that perturb the non-redox-active cofactors of PSII without extracting the manganese cluster. Thus, Yocum and Babcock (*35*) detected $Y_Z^\bullet$ in NH_3-treated thylakoids, and the kinetics of $Y_Z^\bullet$ decay at room temperature in NaCl-treated samples have been studied by Ghanotakis et al. (*34*). Studies by Deak et al. (*30*), Hallahan et al. (*31*) and Andréasson et al. (*33*) also concluded that room temperature accumulation of $Y_Z^\bullet$ is possible in Ca^{2+}- and/or Cl^--perturbed samples. ESE-ENDOR experiments, performed by Britt and co-workers, showed the accumulation of $Y_Z^\bullet$ in acetate-treated samples of *Synechocystis* Y_D-less mutants (*10*).

In contrast, Boussac and Rutherford concluded that the generation of $Y_Z^\bullet$ in Ca^{2+}- and Cl^--depleted samples does not occur (*20*, *32*, *45*). Their room-temperature kinetic EPR study indicates that illumination of inhibited PSII membranes by flashes of 0.25 Hz resulted in no accumulation of $Y_Z^\bullet$ (*20*). However, the data in Figure 4 and Table 1 show that the decay time of the light-induced $Y_Z^\bullet$ in swpr-PSII membranes at room temperature is considerably longer than 4 s. Hence, flashes at 0.25 Hz result in the accumulation of $Y_Z^\bullet$, but its detection as an averaged kinetic trace is not apparent because the dark intervals are too short for the radical to decay. As a consequence, its EPR signal is lost in the base line. Later EPR studies (*32*) on swpr-PSII membranes, in which the amount of spins generated under illumination at nonsaturating EPR conditions was measured, also indicated no light-induced accumulation of $Y_Z^\bullet$. Low microwave power (20 mW) was used to record a tyrosyl signal induced by five flashes, and then a dark-adaptation of 5 min was given before the $Y_D^\bullet$ signal was recorded. With the power used by these investigators, however, the signal-to-noise is very poor and spin counting becomes difficult. Figure 2 shows that saturation occurs at much higher power, so we were able to determine the spins contributing to the dark and light spectra (Figure 3) by using 10 times higher power (200 mW). In addition, 5 min dark-adaptation is probably not sufficient for complete relaxation of the light-induced spins when the 17 and 23 kDa polypeptides are present (Figure 4). For these reasons, we suggest that $Y_Z^\bullet$ was accumulated, but that it escaped detection in the studies reported in (*20*, *32*). Under all conditions we have investigated, illumination of the inhibited samples resulted in about 0.7 spin per PSII. We conclude that the reason for the discrepancies in the literature regarding these issues is the dependence of the kinetic properties of $Y_Z^\bullet$ on the presence of 17 and 23 kDa polypeptides and on the exogenous redox system used experimentally.

The kinetic data presented in Figures 4−6 show biphasic behavior for the $Y_Z^\bullet$ decay. Both phases are sensitive to the extrinsic polypeptide composition of the sample and to the nature of the exogenous redox components added. It is known that the lumenal side of PSII is negatively charged (*54*), which explains the fact that, when ferri- and ferrocyanide are used as the electron acceptor/redox buffer system, $Y_Z^\bullet$ reduction kinetics are slower (see Table 1 and Figures 4 and 5). The negatively charged $[Fe(CN)_6]^{4-}$ ion, which is the electron donor, is repelled by the negative charges on the surface of the membranes, so that its active concentration is much lower than in the bulk. Slow reduction kinetics result. On the other hand, the reduced forms of the hydrophobic and neutral DCBQ and PPBQ can reach $Y_Z^\bullet$ more effectively, and the resulting reduction kinetics are faster. We suspect that the biphasicity in $Y_Z^\bullet$ decay arises from the necessary coupling between protons and electrons in reducing $Y_Z^\bullet$; experiments are currently underway to test this idea. We consider the possibility that the reduced forms of the acceptors provide electrons to the manganese cluster, which then reduces $Y_Z^\bullet$, to be unlikely because, in that case, we would expect very fast $Y_Z^\bullet$ decay kinetics. This is the case when benzidine is used (Figure 8). As originally proposed in (*34*), in the dark between flashes, benzidine reduces the manganese cluster to its lower S-states, which, in turn, reduce the light-induced $Y_Z^\bullet$ rapidly. The experiments presented in Figure 8 reveal the protective role of the 17 and 23 kDa extrinsic polypeptides against reductants, in agreement with the original work by Ghanotakis et al. (*55*). In the absence of these polypeptides, detection of $Y_Z^\bullet$ with the experimental conditions used was not possible. However,

in the presence of 17 and 23 kDa polypeptides, we detected $Y_Z^•$ even at higher benzidine concentrations. The accumulation of oxidizing equivalents as the OEC advances to higher S-states is vital for the catalytic role of PSII in the oxidation of water. Thus, easy access of reductants to OEC must be avoided. We propose that the 17 and 23 kDa polypeptides serve that role on the oxidizing side of PSII, in addition to their well-established role in regulating the Ca^{2+} and Cl^- concentrations.

We examined the decay kinetics of the split signal in samples dark-adapted at 273 K and found that they correlate with the decay of $Y_Z^•$ under similar conditions (Figure 9). We attribute the split signal to $Y_Z^•$ in a magnetic interaction with S_2, in agreement with proposals by Hallahan and co-workers (*31*) and by Britt and co-workers (*4*, *10*). At high temperatures, the EPR signal from the $Y_Z^•$ radical from the inhibited samples is narrow and almost identical with the $Y_D^•$ signal, whereas, at low temperatures, the signal is broadened by the interaction with the paramagnetic S_2-state of the manganese complex. Brudvig and co-workers have attributed the temperature dependence of the $Y_Z^•$ signal shape to the spin−lattice relaxation time (T_1) of the manganese cluster. At ambient temperatures, T_1 is rapid, and the magnetic interaction between the cluster and $Y_Z^•$ is averaged to zero. As a result, the $Y_Z^•$ signal has a narrow line width. At cryogenic temperatures, T_1 is significantly longer, which precludes effective averaging, and the $Y_Z^•$ signal appears broadened. The nature of the magnetic interaction between $Y_Z^•$ and S_2, whether predominantly exchange or predominantly dipolar, is under active debate (*4*, *10*, *43*, *56*). In any case, however, the assignment of the split signal observed at cryogenic temperatures to $Y_Z^•$, which is also present at room temperature, clarifies the nature of the state that accumulates upon illumination of inhibited samples. We found no experimental support for the existence of any radical other than $Y_Z^•$ in magnetic interaction with S_2 in the inhibited PSII membranes. Thus, we suggest that the S_2X state proposed by Junge and co-workers (*21*−*23* and references cited therein) is the same $S_2\ Y_Z^•$ state.

Treatment of O_2-evolving PSII by various reagents (NaCl, acetate, ammonia, citrate) blocks the oxidizing side of the enzyme at the $S_2\ Y_Z^•$ state. The common result of all these treatments is the removal of one or both of the necessary ionic cofactors, Ca^{2+} and Cl^-. Thus, it is important to understand the correlation between the absence of these cofactors and the terminal state reached in these inhibited systems. Recently, a model for water oxidation that postulates hydrogen-atom abstraction from Mn-ligated substrate water by $Y_Z^•$ on each S-state transition has been proposed (*9*, *11*−*13*, *44*). In this model, during each of the first two S-state transitions, $Y_Z^•$ abstracts a hydrogen atom from one substrate water bound to one of the manganese ions of the OEC. With the abstraction of the second H atom, substrate hydrogens in the immediate vicinity of Y_Z are effectively depleted, and some motion, either of protons from substrate water ligated to one of the other manganese ions in the cluster or of Y_Z to the second water substrate, is necessary for further S-state advance. The suggestion was made recently that Cl^- migrates from its Ca^{2+} binding site in the lower S-state to a manganese binding site in S_2 to activate this motion (*12*). This model requires that both Ca^{2+} and Cl^- be present in the active site for a full S-state cycle to occur and that Ca^{2+} must bind prior to Cl^-, consistent with the ordered binding of Ca^{2+} and Cl^- observed earlier by Yocum and co-workers (*57*). In the absence of either cofactor, the observed inhibition at the $S_2\ Y_Z^•$ state is predicted. Recent work by Wincencjusz et al. (*58*) showing that Cl^- is necessary only for the $S_2 \rightarrow S_3$ and $S_3 \rightarrow [S_4] \rightarrow S_0$ transitions is in agreement with this mechanism of action for the non-redox-active cofactors in the OEC.

ACKNOWLEDGMENT

Stimulating discussions with Prof. C. F. Yocum, Dr. C. W. Hoganson, Dr. C. Tommos, and Dr. M. Di Valentin are acknowledged.

REFERENCES

1. Debus, R. (1992) *Biochim. Biophys. Acta 1102*, 269−352.
2. Diner, B. A., and Babcock, G. T. (1996) in *Oxygenic Photosynthesis: The Light Reactions* (Ort, D. R., and Yocum, C. F. Eds.) pp 213−247, Kluwer, Dordrecht, The Netherlands.
3. Ghanotakis, D. F., and Bricker, T. M. (1996) in *Oxygenic Photosynthesis: The Light Reactions* (Ort, D. R., and Yocum, C. F., Eds.) pp 113−136, Kluwer, Dordrecht, The Netherlands.
4. Britt, R. D. (1996) in *Oxygenic Photosynthesis: The Light Reactions* (Ort, D. R., Yocum, C. F., Eds.) pp 137−164, Kluwer Academic Publishers, Dordrecht, The Netherlands.
5. Yachandra, V. K., Sauer, K., and Klein, M. P. (1996) *Chem. Rev. 96*, 2927−2950.
6. Kok, B., Forbush, B., and McGloin, M. (1970) *Photochem. Photobiol. 11*, 457−475.
7. Babcock, G. T., Barry, B. A., Debus, R. J., Hoganson, C. W., Atamian, M., McIntosh, L., Sithole, I., and Yocum, C. F. (1989) *Biochemistry 28*, 9557−9565.
8. Tommos, C., Tang, X.-S., Warncke, K., Hoganson, C. W., Styring, S., McCracken, J., Diner, B. A., and Babcock, G. T. (1995) *J. Am. Chem. Soc. 117*, 10325−10335.
9. Hoganson, C. W., Lydakis-Simantiris, N., Tang, X.-S., Tommos, C., Warncke, K., Babcock, G. T., Diner, B. A., McCracken J., and Styring, S. (1995) *Photosynth. Res. 46*, 177−184.
10. Gilchrist, M. L., Ball, J. A., Randall, D. W., and Britt, R. D. (1995) *Proc. Natl. Acad. Sci. U.S.A. 92*, 9545−9549.
11. Hoganson, C. W., and Babcock, G. T. (1997) *Science 277*, 1953−1956.
12. Tommos, C., and Babcock, G. T. (1998) *Acc. Chem. Res. 31*, 18−25.
13. Lydakis-Simantiris, N., Ghanotakis, D. F., and Babcock, G. T. (1997) *Biochim. Biophys. Acta 1322*, 129−140.
14. Barry, B. A., and Babcock, G. T. (1987) *Proc. Natl. Acad. Sci. U.S.A. 84*, 7099−7103.
15. Debus, R. J., Barry, B. A., Babcock, G. T., and McIntosh, L. (1988) *Proc. Natl. Acad. Sci. U.S.A. 85*, 427−430.
16. Dekker, J. P., van Gorkom, H. J., Wensink, J., and Ouwehand, L. (1984) *Biochim. Biophys. Acta 767*, 1−9.
17. Dekker, J. P. (1992) in *Manganese Redox Enzymes* (Pecoraro, V. L., Ed.) pp 85−103, VCH, New York.
18. Ono, T.-A., Noguchi, T., Inoue, Y., Kusunoki, M., Matsushita, T., and Oyanagi, H. (1992) *Science 258*, 1335−1337.
19. Boussac, A., Zimmermann, J. L., and Rutherford, A. W. (1990) *FEBS Lett. 277*, 69−74.
20. Boussac, A., Sétif, P., and Rutherford, A. W. (1992) *Biochemistry 31*, 1224−1234.
21. Haumann, M., Drevenstedt, W., Hundelt, M., and Junge, W. (1996) *Biochim. Biophys. Acta 1273*, 237−250.
22. Hundelt, M., Haumann, M., and Junge, W. (1997) *Biochim. Biophys. Acta 1321*, 47−60.
23. Haumann, M., Bogershausen, O., Cherepanov, D., Ahlbrink, R., and Junge, W. (1997) *Photosynth. Res. 51*, 193−208.
24. Roelofs, T. A., Liang, W., Latimer, M. J., Cinco, R. M., Rompel, A., Andrews, J. C., Sauer, K., Yachandra, V. K., and Klein, M. P. (1996) *Proc. Natl. Acad. Sci. U.S.A. 93*, 3335−3340.

25. Andrews, J. C., Cinco, R., Dau, H., Latimer, M. J., Liang, W., Roelofs, T. A., Rompel, A., Sauer, K., Yachandra, V. K., and Klein, M. P. (1995) *Physica B 209*, 657−659.
26. Yocum, C. F. (1991) *Biochim. Biophys. Acta 1059*, 1−15.
27. Coleman, W. J. (1990) *Photosynth. Res. 23*, 1−27.
28. Ono, T.-A., Zimmermann, J. L., Inoue, Y., and Rutherford, A. W. (1986) *Biochim. Biophys. Acta 851*, 193−201.
29. Lübbers, K., Drevenstedt, W., and Junge, W. (1993) *FEBS Lett. 336*, 304−308.
30. Deák, S., Vass, I., and Styring, S. (1994) *Biochim. Biophys. Acta 1185*, 65−74.
31. Hallahan, B. J., Nugent, J. H. A., Warden, J. T., and Evans, M. C. W. (1992) *Biochemistry 31*, 4562-4573.
32. Boussac, A., and Rutherford, A. W. (1995) *Biochim. Biophys. Acta 1230*, 195−201.
33. Andréasson, L.-E., Vass, I., and Styring, S. (1995) *Biochim. Biophys. Acta 1230*, 155−164.
34. Ghanotakis, D. F., Babcock, G. T., and Yocum, C. F. (1984) *Biochim. Biophys. Acta 765*, 388−398.
35. Yocum, C. F., and Babcock, G. T. (1981) *FEBS Lett. 130*, 99−102.
36. Boussac, A., and Rutherford, A. W. (1992) *Biochemistry 31*, 7441−7445.
37. Boussac, A., Zimmermann, J.-L., and Rutherford, A. W. (1989) *Biochemistry 28*, 8984−8989.
38. Boussac, A., Zimmermann, J.-L., Rutherford, A. W., and Lavergne, J. (1990) *Nature 347*, 303−306.
39. Sivaraja, M., Tso, J., and Dismukes, G. C. (1989) *Biochemistry 38*, 9559−9464.
40. MacLachlan, D. J., and Nugent, J. H. A. (1993) *Biochemistry 32*, 9972−9980.
41. Szalai, V. A., and Brudvig, G. W. (1996) Biochemistry 35, 1946−1953.
42. Tang, X.-S., Randall, D. W., Force, D. A., Diner, B. A., and Britt, R. D. (1996) *J. Am. Chem. Soc. 118*, 7638−7639.
43. Force, D. A., Randall, D. W., and Britt, R. D. (1997) *Biochemistry 36*, 12062−12070.
44. Babcock, G. T. (1995) in *Photosynthesis: From Light to Biosphere* (Mathis, P., Ed.) Vol. 2, pp 209−215, Kluwer Academic Publishers, Dordrecht, The Netherlands.
45. Boussac, A., and Rutherford, A. W. (1994) *J. Biol. Chem. 269*, 12462−12467.
46. Berthold, D. A., Babcock, G. T., and Yocum, C. F. (1981) *FEBS Lett. 134*, 231−234.
47. Ghanotakis, D. F., Topper, J., Babcock, G. T., and Yocum, C. F. (1984) *Biochim. Biophys. Acta 767*, 524−531.
48. Boussac, A., and Rutherford, A. W. (1988) *Biochemistry 27*, 3476−3483.
49. Piccioni, R., Bellemare, G., and Chua, N.-H. (1982) in *Methods in Chloroplast Molecular Biology* (Edelman, M., Hallick, R. B., & Chua, N.-H., Eds.) pp 985−1014, Elsevier Biomedical Press, Amsterdam, The Netherlands.
50. Warden, J. T., Blankenship, R. E., and Sauer, K. (1976) *Biochim. Biophys. Acta 423*, 462−478.
51. Weil, J. A., Bolton, J. R., and Wertz, J. E. (1994) in *Electron Paramagnetic Resonance, Elementary Theory and Applications*, Wiley & Sons, Inc., New York.
52. Babcock, G. T., Ghanotakis, D. F., Ke, B., and Diner, B. A. (1983) *Biochim. Biophys. Acta 723*, 276−286.
53. Lydakis-Simantiris, N. (1996) Ph.D. Thesis, University of Crete, Greece.
54. Yerkes, C. T., and Babcock, G. T. (1980) *Biochim. Biophys. Acta 590*, 360−372.
55. Ghanotakis, D. F., Topper, J. N., and Yocum, C. F. (1984) *Biochim. Biophys. Acta 767*, 524−531.
56. Szalai, V. A., Kühne, H., Lakshmi, K. V., and Brudvig, G. W. (1997) *J. Am. Chem. Soc.* (submitted for publication).
57. Yocum, C. F. (1992) in *Manganese Redox Enzymes* (Pecoraro, V. L. Ed.) pp 71−83, VCH Publishers, New York.
58. Wincencjusz, H., van Gorkom, H. J., and Yocum, C. F. (1997) *Biochemistry 36*, 3663−3670.
59. Ahlbrink, R., Haumann, M., Cherepanov, D., Bogershausen, O., Mulkidjanian, A., and Junge, W. (1998) *Biochemistry 37*, 1131−1142.

BI972980E